STUDIA UBB CHEMIA, LXII, 4, Tom II, 2017 (p. 495-513)
(RECOMMENDED CITATION)
DOI:10.24193/subbchem.2017.4.42

COMPUTATIONAL INVESTIGATION OF SPECTROSCOPIC PARAMETERS IN PUTATIVE SECONDARY STRUCTURE ELEMENTS FOR POLYLACTIC ACID AND COMPARISON WITH EXPERIMENT

IZABELLA IRSAI[a], ALEXANDRU LUPAN[a], CORNELIA MAJDIK[a], RADU SILAGHI-DUMITRESCU[a]*

ABSTRACT. Putative elements of secondary, tertiary and quaternary structure were examined for polylactic acid chains, attempting a parallel with secondary structure elements known from protein biology and also attempting an estimate, based on accurate atomic-level calculations, of interaction energies between polylactic acid chains. Spectroscopic parameters were predicted for all types of structure examined, in an attempt to aid our on-going efforts in synthesis and characterization of polylactic acid variants.

Keywords: *polylactic acid, secondary structure, NMR, EPR, DFT, semiempirical*

INTRODUCTION

Poly(lactic acid) (PLA) as a biodegradable polymer has a tremendous potential in medical, pharmacological and environmental applications [1-4]. It degrades to nontoxic lactic acid which is naturally present in human body.

PLA homopolymer can crystallize in three polymorphs: α [5-9], β [8,10] and γ [7, 12]. The crystal structures have been studied by X-ray method, the experiments show the presence of 10_3 and 3_1 helical chains of molecules [6,11].

The equimolecular mixture of poly(L-lactic acid) (PLLA) and poly(D-lactic acid) (PDLA) enantiomers has another crystal modification known as the sc-form with 3_1 helices [13-19].

[a] *Babeş-Bolyai University, Faculty of Chemistry and Chemical Engineering, 11, Arany Janos Street, RO-4000228 Cluj-Napoca, Romania*
** Corresponding author: rsilaghi@chem.ubbcluj.ro*

The crystal structures were also analyzed by computational chemistry. The poly(lactic acid) polymorphs were studied by rotational isomeric state models [20, 21], molecular dynamics [9, 10], Monte Carlo models [21,22], molecular mechanics [9] and quantum chemical [23-25] simulations. It was found that neither a pre 10_3 nor 3_1 helix could fit the experimental data perfectly, suggesting a certain degree of disorder in the structure.

RESULTS AND DISCUSSION

Four secondary-types structure were optimized – helical structures (α, π, 10_3) and β-sheet – employing molecular mechanics, semiempirical, ab initio and density functional methods. The highest-level method (DFT/M062x) denotes that the α, π and 10_3 structures have very similar energies, with π slightly favored by values, this in a contrast with results obtained with less accurate semiempirical and empirical methods, which predict larger differences and other structures as favorites.

Figure 1 shows optimized geometries for models of polylalctic acid (PLA) employed in the present study. Decameric structures of L-lactic acid (PLLA) as well as of alternating D,L monomers (PDLLA) were employed. Details of these structures and their relative energies are described elsewhere. The energy in the case of PLLA are generally smaller than in the case of PDLLA, suggesting that such structures are more stable.

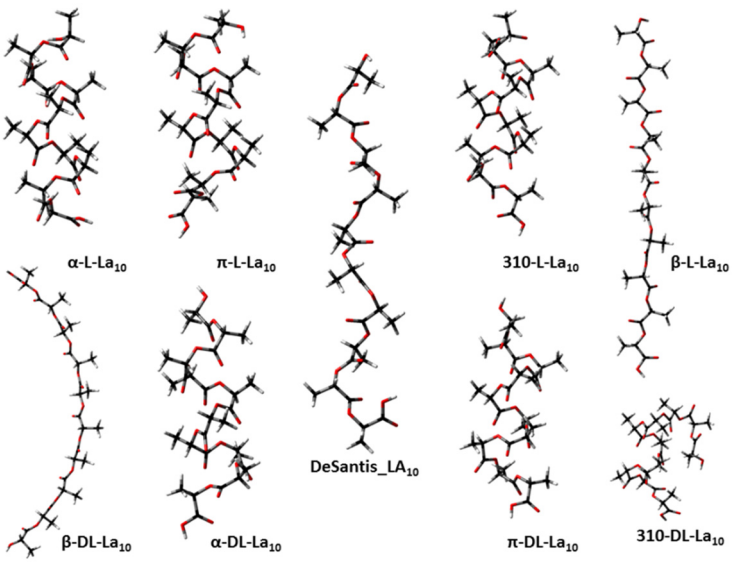

Figure 1. Graphical representation of polylactic acid geometries optimized by DFT

The vibrational frequencies were computed for these optimized structures. In addition it was calculated the vibrational frequencies of the polylactic structure described by DeSantis.

The IR spectra shows characteristic bands mainly due to methylene and carboxylic C=O bonds. A repeat unit of PLA consists of three skeletal bonds: C-O, O-C_α, C_α-C. For PLA the bands are assigned due to backbone bond stretching (C-O, O-C_α, C-C_α,), backbone bond angle bending (O-C-C_α, C-O-C_α, O-C_α-C), for the side branches the bending (O-C_α-C_β, C-C_α-C_β, C_α-C=O) and stretching (C_α-C_β, C=O).

Figure 2 shows the IR spectrum of polylactic acid prepared as described in the Methods section. It can be seen the bands of C=O stretching (1751,20 cm^{-1}), C-OC stretching (1117,42 cm^{-1}) and CH bending and C-OC stretching (1064,37 cm^{-1}).

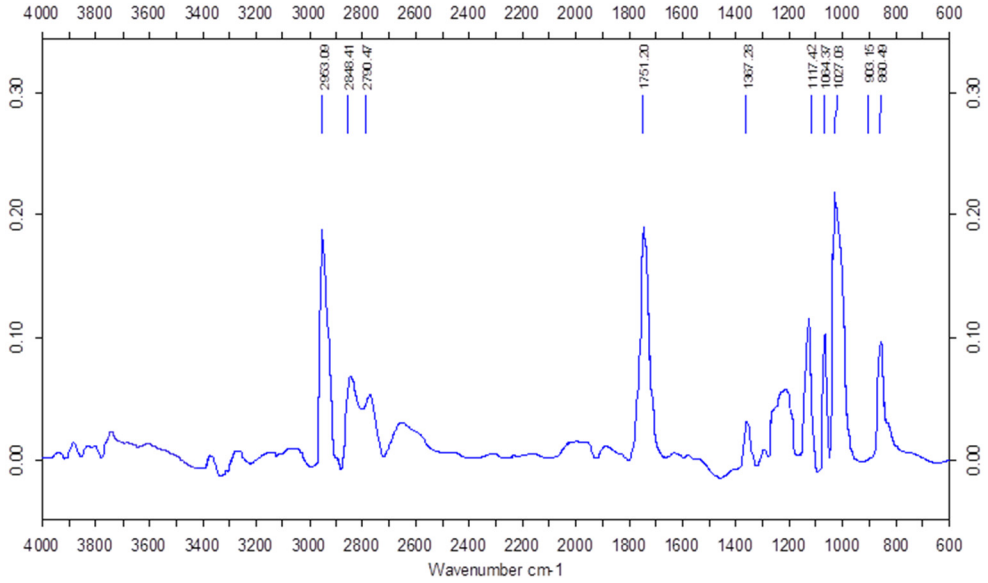

Figure 2. IR spectrum of poly(L-lactic acid) (cf. Materials and Methods)

Figure 3 shows computed IR spectra for the five secondary structure elements considered in the present work. The intensity of IR vibrations depend on the structure of the poly(lactic acid).

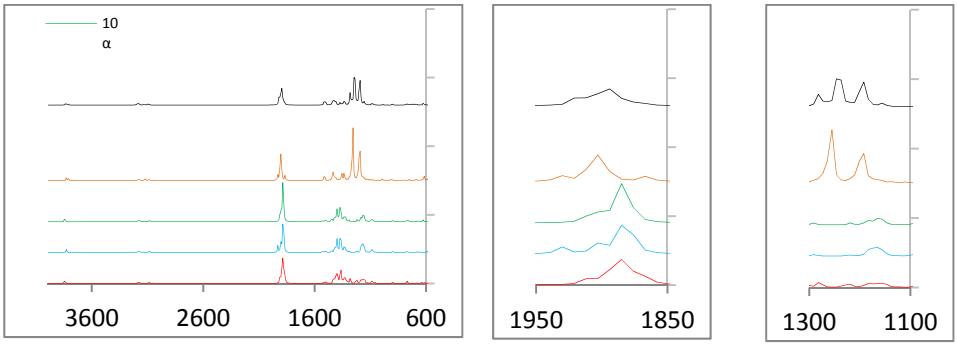

Figure 3. IR spectra of PLLA (M062x/6-31G**):(a) full spectrum; (b) carbonyl stretching region; (c) backbone stretching region

The IR spectra of the five structures show the same number of bands. The solvation does not involve any additional band.

The bands below 225 cm-^{1} are mainly due to the skeletal torsion. The 225-925 cm^{-1} region bands are assigned due to the bending of the side branches. There are no significant intensities.

The CH_3 is responsible for the appearance of the band in the 925-1110 cm^{-1} region due to the rocking vibrations. The solvation increases the intensities in the case of the three helical structures.

The C-CH_3 and C-OC stretching cause the presence of bands in the 1124-1213 cm^{-1} backbone stretching region. The intensities of the bands corresponding to C-CH_3 stretch are medium in the case of the helical structures, the water double these values. The β-sheet and the structure described by DeSantis provide weak bands. C-OC stretching band are shown in 1151-1217 cm^{-1} region. Assignment of the β-sheet is the most intensive, six times higher than the others. The solvation increases the intensity further. The structure described by DeSantis has a strong band in this region.

In the 1215-1412 cm^{-1} region it can be seen bands assigned to CH, CH_3 bending and C-O-C stretching. The intensity of the CH bending and C-O-C stretching in the case of β-sheet and the structure described by DeSantis are very strong in contrast with the helical structure. These are the highest intensity bands in the entire spectrum. The water does not influence these intensities. The CH bending intensities are roughly the same with the exception of structure described by DeSantis. The solvation increases the

intensities in the case of the helical structures. A different medium band appear in this region due to the CH bending and CH_3 scissoring. It is worth noting the assignments in the 1407-1437 cm^{-1} region. In this interval appear the bands due to CH_3 scissoring vibrations. In the case of the three helical structures are not significant intensities, but in the case of β-sheet the intensity is notable.

IR spectra of the PLLA in the range of 1865-1932 cm^{-1} appear to be distinct for each of the five conformations. There is not much difference between the C=O stretching intensities calculated by DFT/M062x/6-31G** method. In turn the solvation increases the intensities in all five structures. The five conformers exhibit single absorption bands, spaced by about 9 and 18 cm^{-1} from each other.

The CH stretching, the symmetric and asymmetric stretching of CH3 result the appearance of weak bands in the 3050-3191 cm^{-1} CH spectral region. It can be seen that the stretching frequencies are higher than the corresponding bending frequencies.

The calculated frequencies (cm^{-1}) and peak band assignment for the helical structures and β-sheet of PLLA are shown in tables 1-4.

In order to demonstrate that the chain conformation changes the interval of IR frequencies it was calculated the IR spectra of PDLLA and then compared to experimental data. Figure 4. shows the IR spectrum of PDLLA. The spectrum represent the bands of CH bending and C-OC stretching (1088 cm^{-1}), C-OC stretching (1188 cm^{-1}), C=O stretching (1752 cm^{-1}), CH_3 symmetric stretching (2945 cm^{-1}), CH_3 asymmetric stretching (2997 cm^{-1}) and OH stretching (3737 cm^{-1}).

In the IR spectra of PDLLA it can be seen the same bands as in the case of PLLA. The bands below 900 cm^{-1} represent weak intensities. The CH_3 rocking and C-CH_3 stretching band intensities decrease slightly compared to PLLA. The C-OC stretching's bands appear at lower values (1146-1215 cm-1) than in the case of PLLA. The intensities of the α helix and the β-sheet increase significantly. The calculated intensity of assignment of β-sheet is bigger in vacuum than in the solvated model.

The CH bending and C-OC stretching bands have equivalent values in the 1204-1325 cm^{-1} interval, but bigger than the PLLA's one; the β-sheet and the structure described by DeSantis bands' intensities are 5-8 higher than in the case of the helices. It was observed that intensities of β-sheet in vacuum and solvation show outstanding values over the others, but these values are much smaller than in the case of PLLA.

Table 1. Peak band assignments for α-L-LA_{10}

α-L-LA_{10}				
M062X 6-31G**		M062X 6-31G** water		
v(cm^{-1})	Intensity	v(cm^{-1})	Intensity	Assignment
18-224	0-6	13-216	0-9	skeletal torsion
233-296	0-6	224-266	0-12	CH_3 rocking
302-399	0-48	299-394	0-73	CH_3 wagging
402	147	399	216	OH (free) bending
407-411	32-59	401-405	32-88	CH_3 wagging
413	63	406	88	OH (free) bending
416-558	1-18	409-592	0-148	CCO bending
627	91	631	116	OH (COOH) bending
663-789	1-34	663-787	1-38	C=O bending
848	7	841	11	C-CO (carboxyl) stretching
879-909	1-31	880-908	2-37	CH_3 bending + COC bending
925-1105	1-107	924-1096	1-238	CH_3 rocking
1127-1164	13-105	1120-1155	11-220	C-CH_3 stretching
1167-1189	5-82	1158-1182	2-127	C-OC stretching
1218-1331	1-118	1217-1330	31-228	CH bending + C-OC stretching
1336-1373	1 -328	1331-1366	13-1022	CH bending
1376-1406	10- 287	1367-1402	17-303	CH bending + CH_3 scissoring
1417-1427	2-53	1409-1421	3-65	CH_3 scissoring
1447	19	1434	104	CH_3 twisting (COOH end)
1448	159	1439	148	CH_3 twisting (OH end)
1494-1532	1-19	1483-1516	3-22	CH_3 twisting
1876-1909	30 -947	1854-1885	72-1580	C=O stretching
3074-3094	7-10	3078-3089	9-18	CH_3 sym stretching
3110-3153	1 -9	3140-3152	2-15	CH stretching
3162-3196	1-16	3164-3196	1-25	CH_3 asym stretching
3839	61	3817	155	OH (free) stretching
3846	94	3820	96	OH (COOH) stretching

The intensities of the bands appearing in the IR spectra due to CH bending are much smaller in all five structures than the corresponding bands of PLLA. The band caused by CH bending and CH_3 scissoring vibrations have the same intensity, with the exception the β-sheet.

The values of the CH_3 scissoring vibrations show tremendous growth relative to PLLA. In the C=O stretching region the bands are very strong, but they are slightly smaller than the corresponding values in PLLA. The

solvation increases importantly the intensities of CH bending and C-OC stretching and C=O stretching vibrations. In the 1815-1935 cm^{-1} region are the C=O stretching bands of PDLLA. The greatest intensity is shown by the β-sheet calculated in the solvated model.

Table 2. Peak band assignments for 3_{10}-L-LA_{10}

3_{10}-L-LA_{10}				
M062X 6-31G**		M062X 6-31G** water		
v(cm^{-1})	Intensity	v(cm^{-1})	Intensity	Assignment
19-226	0-11	17-214	0 -8	skeletal torsion
234-281	0-14	219-286	0-9	CH_3 rocking
299-400	0-58	295-396	0-170	CH_3 wagging
409	22	399	141	OH (free) bending
410-416	9-40	403-406	4-8	CH_3 wagging
419	4	407	5	OH (free) bending
425-588	1-230	410-596	1-135	CCO bending
636	70	644	63	OH (COOH) bending
655-788	0-35	660-775	0-50	C=O bending
824	14	842	21	C-CO (carboxyl) stretching
878-910	1-45	891-909	1-37	CH_3 bending + COC bending
925-1106	1-93	925-1099	0-217	CH_3 rocking
1127-1164	15-106	1104-1161	41-232	C-CH_3 stretching
1167-1189	5-146	1162-1185	3-213	C-OC stretching
1222-1331	3-89	1213-1329	8-369	CH bending + C-OC stretching
1332-1372	11-403	1331-1365	4-938	CH bending
1373-1403	6-182	1367-1402	11-311	CH bending + CH_3 scissoring
1412-1426	3-88	1407-1421	12-80	CH_3 scissoring
1445	28	1430	1430	CH_3 twisting (COOH end)
1448	83	1445	120	CH_3 twisting (OH end)
1495-1528	0-46	1486-1518	1-33	CH_3 twisting
1875-1931	32-756	1852-1894	57-1074	C=O stretching
3078-3094	7-10	3071-3091	9-17	CH_3 sym stretching
3115-3152	1-9	3120-3154	4-13	CH stretching
3171-3193	0-14	3159-3194	2 -25	CH_3 asym stretching
3826	62	3850	75	OH (free) stretching
3830	100	3807	159	OH (COOH) stretching

Table 3. Peak band assignments for π-L-LA_{10}

π-L-LA_{10}				
M062X 6-31G**		M062X 6-31G** water		
v(cm^{-1})	Intensity	v(cm^{-1})	Intensity	Assignment
18-225	0-6	10-222	0-6	skeletal torsion
239-286	0-66	229-291	1-12	CH_3 rocking
290-398	0 -66	296-393	1-157	CH_3 wagging
403	22	398	47	OH (free) bending
408-411	7-26	400-403	3-81	CH_3 wagging
414	6	406	23	OH (free) bending
420-587	2 -34	410-586	1-87	CCO bending
611	73	606	95	OH (COOH) bending
640-790	1-71	638-789	2-78	C=O bending
832	5	835	8	C-CO (carboxyl) stretching
894-915	0-47	890-911	12-70	CH_3 bending + COC bending
928-1102	0-91	927-1097	2-240	CH_3 rocking
1124-1165	8-85	1106-1157	45-233	C-CH_3 stretching
1166-1217	9-150	1163-1186	8-127	C-OC stretching
1231-1330	11-192	1216 -1334	22-320	CH bending + C-OC stretching
1334-1373	6-416	1335-1365	21-586	CH bending
1378-1411	6-222	1368-1407	6-291	CH bending + CH_3 scissoring
1417-1433	6-104	1409-1426	9-104	CH_3 scissoring
1436	53	1431	110	CH_3 twisting (COOH end)
1451	3	1432	121	CH_3 twisting (OH end)
1494-1530	2-20	1487-1513	0-29	CH_3 twisting
1865-1910	34-999	1854-1878	56-1313	C=O stretching
3050-3090	6-32	3080-3098	9-21	CH_3 sym stretching
3093-3154	0-11	3100-3151	2-15	CH stretching
3170-3191	1-12	3166-3201	1-24	CH_3 asym stretching
3835	53	3854	72	OH (free) stretching
3846	98	3821	155	OH (COOH) stretching

CH3 scissorings cause bands in 1409-1438 cm^{-1} region. The intensities are medium, with the solvated β-sheet showing larger values.

The calculated frequencies (cm^{-1}) and peak band assignment for the helical structures and β-sheet of PDLLA are shown in tables 5-8.

Table 4. Peak band assignments for β-L-LA_{10}

β-L-LA_{10}				
M062X 6-31G**		M062X 6-31G** water		
ν(cm^{-1})	Intensity	ν(cm^{-1})	Intensity	Assignment
5-202	0-31	5-203	0-36	skeletal torsion
220-313	0-18	208-301	0-145	CH_3 rocking
317	65	314	8	OH (free) bending
327-402	0-18	329-397	1-26	CH_3 wagging
421-579	0-38	416-578	0-62	CCO bending
587	79	593	102	OH (COOH) bending
602-801	0-40	601-799	2-134	C=O bending
844	13	844	14	C-CO (carboxyl) stretching
896-912	1-22	894-909	2-36	CH_3 + COC bending
932-1110	0-54	928-1106	0-49	CH_3 rocking
1130-1145	1-20	1124-1143	0-47	C-CH_3 stretching
1157-1213	23-970	1151-1187	3-2171	C-OC stretching
1215-1290	4-3164	1213-1286	3-3093	CH bending + C-OC stretching
1318-1370	1-378	1316-1366	1-341	CH bending
1375-1412	1-83	1369-1407	2-54	CH bending + CH_3 scissoring
1414-1437	4-332	1408-1433	8-455	CH_3 scissoring
1447	76	1444	109	CH_3 twisting (COOH end)
1468	5	1459	9	CH_3 twisting (OH end)
1508-1518	5-55	1495-1509	2-75	CH_3 twisting
1865-1932	9-563	1850-1898	4-1293	C=O stretching
3058-3095	5-23	3076-3104	8-22	CH_3 sym stretching
3117-3130	5-22	3125-3134	8-16	CH stretching
3169-3196	3-14	3163-3196	7-25	CH_3 asym stretching
3829	112	3819	103	OH (free) stretching
3810	81	3806	169	OH (COOH) stretching

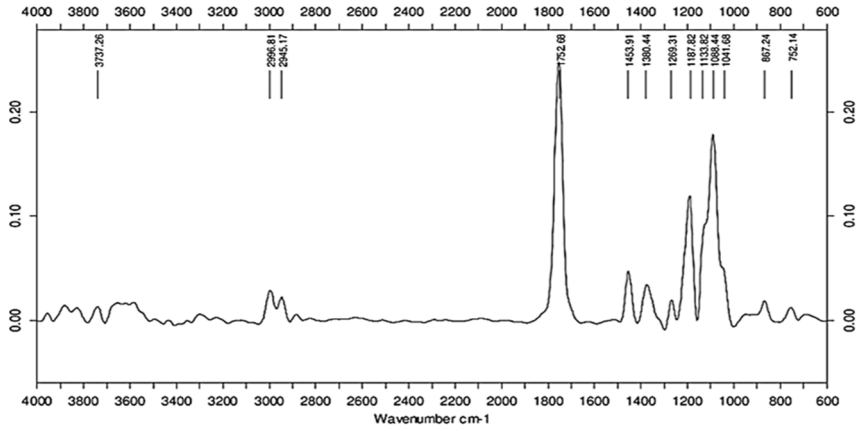

Figure 4. IR spectrum of poly(DL-lactic acid).

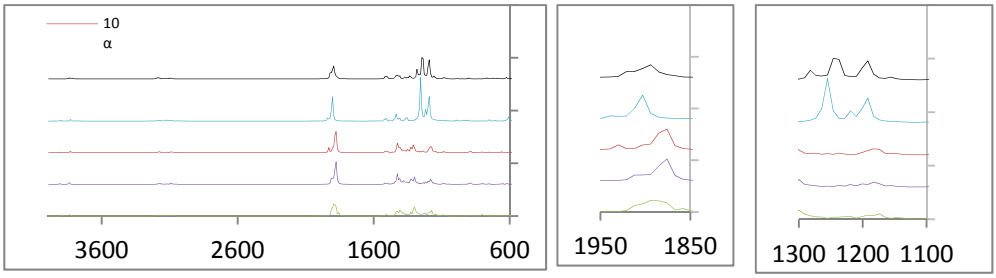

Figure 5. IR spectra of PDLLA (M062x/6-31G**):(a) full spectrum; (b) carbonyl stretching region; (c) backbone stretching region

Table 5. Peak band assignments for α-DL-LA_{10}

α-DL-LA_{10}				
M062X 6-31G**		M062X 6-31G** water		
v(cm^{-1})	Intensity	v(cm^{-1})	Intensity	Assignment
8-190	0-6	13-189	0-9	Skeletal torsion
199-241	0- 44	201-237	0-5	CH_3 rocking
242	56	238	1-5	OH (free) bending
246-290	1-7	241-294	0-18	CH_3 rocking
302-408	0-26	298-422	1-156	CH_3 wagging
428-580	1-47	427-567	2-96	CCO bending
585	41	576	63	OH (COOH) bending
593-807	0-57	603-802	1-87	C=O bending
819	22	821	37	C-CO (carboxyl) stretching
881-900	3-56	881-900	2-63	CH_3 bending + COC bending
923-1092	1-35	923-1087	1-71	CH_3 rocking
1139-1168	3-39	1130-1164	10-90	C-CH_3 stretching
1175-1199	12-296	1167-1198	17-289	C-OC stretching
1232-1323	10-320	1225-1324	22-838	CH bending + C-OC stretching
1327-1380	7-163	1326-1374	17-258	CH bending
1383-1416	13-147	1378-1412	7-294	CH bending + CH_3 scissoring
1419-1429	7-287	1414-1424	14-230	CH_3 scissoring
1436	29	1437	62	CH_3 twisting (COOH end)
1464	31	1451	40	CH_3 twisting (OH end)
1492-1528	0-35	1481-1515	1-30	CH_3 twisting
1871-1930	42-875	1854-1888	127-1047	C=O stretching
3039	28	3029	40	CH stretching
3073-3101	3-17	3082-3102	4-20	CH_3 sym stretching
3111-3137	1-13	3115-3150	5-11	CH stretching
3153-3213	1-26	3167-3209	2-25	CH_3 asym stretching
3907	48	3882	78	OH (free) stretching
3830	103	3809	160	OH (COOH) stretching

Table 6. Peak band assignments for 10_3-DL-LA_{10}

10_3-DL-LA_{10}				
M062X 6-31G**		M062X 6-31G** water		
v(cm^{-1})	Intensity	v(cm^{-1})	Intensity	Assignment
15-203	0-6	23-184	0-8	Skeletal torsion
211-248	0-73	191-227	0-3	CH_3 rocking
249	0-6	23-184	0-8	OH (free) bending
252-292	1-5	236-291	1-10	CH_3 rocking
295-420	0-17	298-420	2-192	CH_3 wagging
428-572	2-39	431-560	3-105	CCO bending
581	10	564	28	OH (COOH) bending
604-808	0-76	601-798	0-141	C=O bending
826	10	814	21	C-CO (carboxyl) stretching
882-903	2-43	867-889	1-135	CH_3 bending + COC bending
924-1093	1-28	911-1080	1-123	CH_3 rocking
1138-1171	1-40	1111-1141	31-258	C-CH_3 stretching
1174-1202	13-120	1146-1177	10-264	C-OC stretching
1218-1325	28-455	1204-1313	62-1119	CH bending + C-OC stretching
1330-1384	7-203	1316-1368	11-286	CH bending
1385-1419	11-139	1369-1407	4-310	CH bending + CH_3 scissoring
1421-1429	7-248	1410-1418	13-40	CH_3 scissoring
1443	115	1428	66	CH_3 twisting (COOH end)
1464	37	1444	28	CH_3 twisting (OH end)
1496-1533	0-26	1486-1513	6-20	CH_3 twisting
1871-1910	62-672	1815-1840	31-1034	C=O stretching
3052	26	3045	34	CH stretching
3073-3096	3-21	3071-3097	8-15	CH_3 sym stretching
3108-3141	2-8	3117-3155	2-22	CH stretching
3154-3215	0-25	3158-3196	1-22	CH_3 asym stretching
3839	104	3764	159	OH (COOH) stretching
3907	50	3854	76	OH (free) stretching

Comparing the calculated data with the experimental data it can be seen that the calculated frequency values are bigger than the experimental values.

Table 7. Peak band assignments for π-DL-LA_{10}

π-DL-LA_{10}				
M062X 6-31G**		M062X 6-31G** water		
v(cm^{-1})	Intensity	v(cm^{-1})	Intensity	Assignment
15-200	0-5	14-186	0-10	Skeletal torsion
202-247	0-3	192-236	0-7	CH_3 rocking
249	3	240	4	OH (free) bending
253-290	1-53	242-296	0-21	CH_3 rocking
304-405	1-26	298-409	1-97	CH_3 wagging
437-565	3-36	410-568	2-59	CCO bending
585	11	572	15	OH (COOH) bending
588-805	1-72	596-803	1-141	C=O bending
832	9	825	48	C-CO stretching
879-903	2-25	857-902	0-43	CH_3 bending + COC bending
923-1099	1-32	923-1087	1-96	CH_3 rocking
1134-1169	4-59	1125-1163	11-144	C-CH_3 stretching
1171-1199	31-144	1167-1196	36-185	C-OC stretching
1221-1323	20-433	1209-1323	24-1048	CH bending+ C-OC stretching
1329-1379	6-177	1331-1372	11-213	CH bending
1386-1417	14-209	1377-1412	12-178	CH bending + CH_3 scissoring
1421-1438	1161-101	1413-1429	6-236	CH_3 scissoring
1440	40	1437	106	CH_3 twisting (COOH end)
1466	18	1454	33	CH_3 twisting (OH end)
1488-1526	3-20	1482-1516	2-32	CH_3 twisting
1856-1910	29-531	1854-1881	87-886	C=O stretching
3066	12	3031	40	CH stretching
3084-3102	3-15	3081-3101	4-19	CH_3 sym stretching
3109-3154	2-9	3118-3153	5-14	CH stretching
3163-3210	1-29	3167-3208	2-22	CH_3 asym stretching
3893	51	3882	79	OH (free) stretching
3836	102	3815	156	OH (COOH) stretching

Table 8. Peak band assignments for β-DL-LA_{10}

β-DL-LA_{10}				
M062X 6-31G**		M062X 6-31G** water		
v(cm^{-1})	Intensity	v(cm^{-1})	Intensity	Assignment
4-197	0-47	5-194	0-41	Skeletal torsion
212-244	0-7	208-240	0-4	CH_3 rocking
248	23	244	2	OH (free) bending
256-318	1-11	249-316	0-161	CH_3 rocking
329-389	0-16	320-384	1-22	CH_3 wagging
396-600	0-71	390-602	0-102	CCO bending
607	205	615	24	OH (COOH) bending
613-808	1-45	616-803	1-224	C=O bending
844	11	846	14	C-CO (carboxyl) stretching
896-912	2-43	891-908	1-29	CH_3 bending + COC bending
931-1105	1-46	926-1104	1-93	CH_3 rocking
1126-1146	1-24	1121-1140	2-32	C-CH_3 stretching
1152-1215	9-1571	1147-1201	5-1311	C-OC stretching
1217-1286	1-2570	1211-1283	3-2270	CH bending + C-OC stretching
1295-1367	7-166	1301-1363	13-150	CH bending
1367-1411	1-102	1365-1406	0-80	CH bending + CH_3 scissoring
1412-1435	1-254	1409-1435	1-403	CH_3 scissoring
1445	88	1449	102	CH_3 twisting (COOH end)
1454	37	1452	55	CH_3 twisting (OH end)
1507-1523	3-37	1495-1516	6-57	CH_3 twisting
1900-1935	24-888	1870-1901	5-2423	C=O stretching
3042	28	3065	34	CH stretching
3075-3092	5-15	3077-3094	8-321	CH_3 sym stretching
3114-3125	9-13	3128-3137	5-27	CH stretching
3156-3198	0-20	3162-3199	7-23	CH_3 asym stretching
3827	110	3797	170	OH (COOH) stretching
3903	39	3887	81	OH (free) stretching

NMR

Another important tool to characterize the structure of the polymer is the NMR spectroscopy. It was used ^1H NMR and ^{13}C NMR spectroscopy. In the ^1H NMR spectra the determined chemical shifts correspond to CH and CH_3 resonance. CO, CH_3 and CH resonance are found in ^{13}C NMR spectra. The ^1H NMR spectra of the PDLLA obtained by polycondensation of DL-lactic acid is shown in figure 6. The NMR analysis of poly(lactic acid) were found

considerably improved by recording spectra in DMSO-d_6 instead of $CDCl_3$ [27].The most intensive signals were those located at 1.45 and 4.93 respectively 1.46 and 5.16 ppm which correspond to CH and CH_3 resonance in PLLA respectively PDLLA.

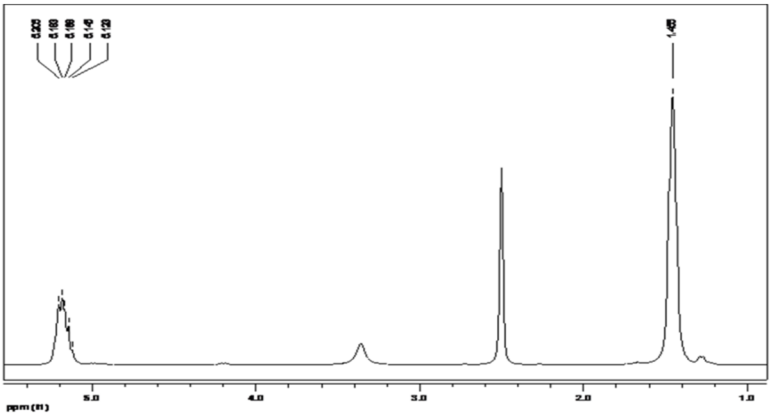

Figure 6. ^{1}H-NMR spectrum of PDLLA.

The simulated ^{1}H NMR spectrum of PLLA is shown in figure 7.

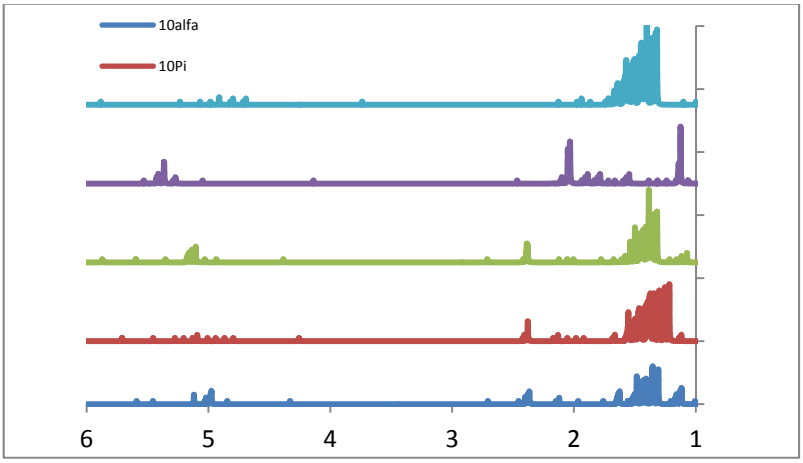

Figure 7. ^{1}H NMR spectra of PLLA (M062x/6-31G**).

The shifts of ^{13}C NMR spectrum of the four secondary-type structure of PLLA calculated by DFT/M062x/6-31G** method are larger than those calculated in solvated models (Table 9.). The ^{1}H NMR chemical shifts of PLLA are not always smaller in solution (Table 10.). Taking into account all five NMR signals covered by these two Tables, the β and π structures appear to generally yield the closest values to the experiment.

Table 9. Computed and experimental ^{13}C NMR Chemical shifts (δ, in ppm) of CO, CH and CH_3 of PLLA in vacuum (v) and water (w), respectively

PLLA	α		π		10_3		β		Exp.
	v	w	v	w	v	w	v	w	
δ (CO)	178	175	178	175	177	175	175	172	172
δ (CH)	72	68	72	68	72	68	72	67	66
δ (CH_3)	19	13	19	13	18	13	19	14	17

Table 10. Computed and experimental ^{1}H NMR Chemical shifts (δ, in ppm) of CH and CH_3 of PLLA in vacuum (v) and water (w), respectively

PLLA	α		π		10_3		β		Exp.
	v	w	v	w	v	w	v	w	
δ (CH)	5.2	5.1	5.1	5.1	5.2	5.1	5.3	5.5	4.9
δ (CH_3)	1.7	1.7	1.7	1.6	1.7	1.7	1.7	1.6	1.5

Figure 8 shows the calculated ^{1}H NMR spectrum of PDLLA.

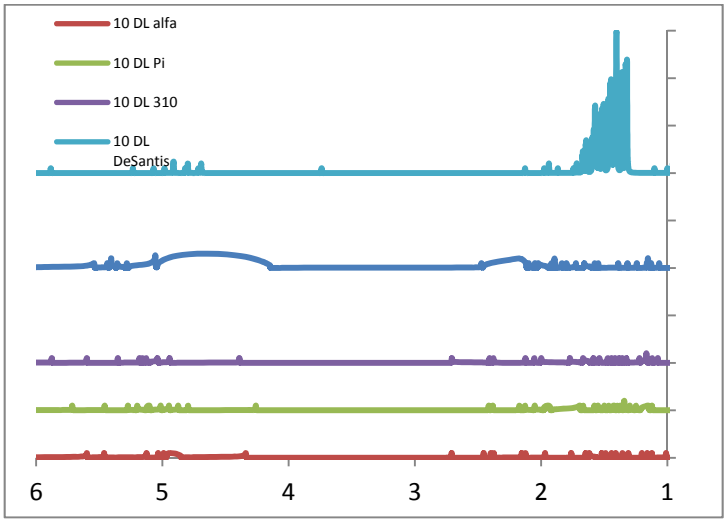

Figure 8. ^{1}H NMR spectra of PDLLA (M062x/6-31G**).

Same as in the case of PLLA the chemical shifts of ^{13}C NMR spectrum of PDDLA show smaller values in solvated model (Table 11.). The ^{1}H NMR shifts due to CH resonance are bigger in all four structures (Table 12.).

Table 11. ^{13}C NMR Chemical shifts (δ, in ppm) of CO, CH and CH_3 of PDLLA in vacuum (v) and water (w), respectively

PDLLA	α		π		10_3		β		Exp.
	v	w	v	w	v	w	v	w	
δ (CO)	177	174	177	174	178	176	175	172	169
δ (CH)	73	68	73	69	73	67	71	67	69
δ (CH_3)	18	13	18	13	18	13	19	14	16

Table 12. ^{1}H NMR Chemical shifts (δ, in ppm) of CH and CH_3 of PDLLA in vacuum (v) and water (w), respectively

PDLLA	α		π		10_3		β		Exp.
	v	w	v	w	v	w	v	w	
δ (CH)	5.0	5.1	5.1	5.1	5.1	5.1	5.4	5.5	5.2
δ (CH_3)	1.7	1.7	1.6	1.6	1.7	1.6	1.5	1.6	1.5

The NMR spectra of PLA can give information about the stereochemistry of the composition. The CO chemical shifts are larger in the α, π and β forms of PLLA, while the CH_3 shifts are larger in the case of the three helical structures of PLLA. The chemical shifts of ^{1}H NMR spectra of PLLA show larger values in all cases except the CH shifts of β-sheet.

CONCLUSIONS

Geometry optimization performed on polylactic acid at different levels of DFT methods suggest that the most stable of the four structures is the π helix and the least stable is the β sheet.

The calculated chemical shifts of both ^{13}C NMR and ^{1}H NMR are slightly larger than the experimental one. The solvation reduces the value of the NMR chemical shifts.

The secondary structure of poly(lactic acid) cannot be conclusively clarified from the calculated IR and NMR spectra, suggesting either a need for using more appropriate computational methods or the occurrence of previously unconsidered elements of secondary structure, or the total lack thereof.

EXPERIMENTAL SECTION

Materials. Aqueous solutions of L-(+)-lactic acid from Sigma-Aldrich (80%), DL-lactic acid from Fluka (90%) were used. PLLA and PDLLA were synthetized by direct dehydropolycondensation. Lactic acid, toluene and 0.1% tin(II) 2-ethylhexanoate catalyst were mixed into a reaction vessel equipped with a Dean-Stark-type condenser, and heated to the refluxing temperature of the solvent. The reaction time was 20 h. The final product was dissolved in chloroform and precipitated in diethyl ether for purification. The polymer was then filtered out from diethyl ether and dried under vacuum.

Measurements. NMR spectra were recorded with a Bruker Avance 300 spectrometer at the following frequencies: ^{1}H, 300.13 MHz; ^{13}C, 75.47 MHz (reference TMS) with DMSO-d_6 as the sovent. IR spectra were recorded with a Vector 22 Bruker spectrometer by direct introduction method and a Jasco FT/IR Specord 600 spectometer in KBr pills. The molecular weights were determined by MALDI-TOF MS (Matrix Assisted Laser Desorption Ionization) analysis with a Bruker BIFLEX III^{TM} spectrometer.

Molecular simulation. A vibrational analysis and NMR simulation has been carried out to analyze the secondary structure of poly(lactic acid) resulted from esterification of ten lactic acid units, hereafter referred to as LA_{10}. These models were built in the Hyperchem [28] software package using built-in options of the Editor module for creating helical structures as well as sheet. Spectroscopic parameters were predicted for helical (α, π, 103) and β-sheet structures, in an attempt to aid our on-going efforts in the synthesis and characterization of poly(lactic acid) variants.

The methods tested here include density functional (M062X/6-31G*, M062X/6-31G**, solvated M062X/6-31G**) applied with standard convergence criteria as defined in Gaussian 09 [29]. Spectral parameters were invoked using the commands Freq and NMR. In terms of the importance of solvation, this is estimated by comparing values computed in water (as a limit of very polar medium) and vacuum (as a limit of completely non-polar medium). Further detail on geometry optimizations and on relative energies of the structures are given elsewhere [30].

ACKNOWLEDGMENTS

This work was supported by CNCSIS-UEFISCDI, projects PNII – ID 312/2008 (RSD and AL), project Parteneriate 72152/2008 (to CM) and by a PhD scholarship from Contract POSDRU/88/1.5/S/60185 – “Innovative doctoral studies in a knowledge based society” (to II).

REFERENCES

1. R.A. Jain, *Biomaterials*, **2000**, 21, 2475.
2. A. Dev, N.S. Binulal, A. Anitha, S.V. Nair, T. Furuike, H. Tamura, R. Jayakumar, *Carbohydrate Polymers*, **2010**, 80, 833.
3. M.A. Ibrahim, A. Ismail, M.I. Fetou, A. Gopferich, *Journal of Controlled Release*, **2005**, 106, 241.
4. S. Fredenberg, M. Wahlgren, M. Reslow, A. Axelsson, *International Journal of Pharmaceutics,* **2011**, 415, 34.
5. T. Miyata, T. Masuko, *Polymer*, **1997**, 38, 4003.
6. J. Kobayashi, T. Asahi, M. Ichiki, A. Okikawa, H. Suzuki, T. Watanabe, E. Fukada, Y. Shikinami, *Journal of Applied Physics*, **1995**, 77, 2957.
7. W. Hoogsteen, A.R. Postema, A.J. Pennings, G.G ten Brinke, P. Zugenmaier, *Macromolecules,* **1990**, 23, 634.
8. S. Sasaki, T. Asakura, *Macromolecules*, **2003**, 36, 8385.
9. D. Brizzolara, H.J. Cantow, K. Diederichs, E. Keller, A.J. Domb, *Macromolecules,* **1996**, 29, 191.
10. C. Aleman, B. Lotz, J. Puiggali, *Macromolecules*, **2001**, 34, 4795.
11. P. De Santis, J. Kovacs, *Biopolymers*, **1968**, 6, 299.
12. J. Puiggali, Y. Ikada, H. Tsuji, L. Cartier, T. Okihara, B. Lotz, *Polymer*, **2000**, 41, 8921.
13. T. Okihara, M. Tsuji, A. Kawagushi, K.I. Katayama, H. Tsuji, S.H. Hyon, Y. Ikada, *Journal of Macromolecular Science Physics B*, **1991**, 30, 119.
14. L. Cartier, T. Okihara, Y. Ikada, H. Tsuji, J. Puiggali, B. Lotz, *Polymer*, **2000**, 41, 8909.
15. Y. Ikada, K. Jamshidi, H. Tsuji, S.H. Hyon, *Macromolecules*, **1987**, 20, 904.
16. H. Tsuji, *Macromolecular Biosc*ience, **2005**, 5, 569.
17. H. Tsuji; Y. Ikada, *Polymer*, **1999**, 40, 6699.
18. H. Tsuji, I. Fukui, *Polymer*, 2003, 44, 2891.
19. D. Sawai, Y. Tsugane, M. Tamada, T. Kanamoto, M. Sungil, S.H. Hyon, *Journal Polymer Science, Part B: Polymer Physics*, **2007**, 45, 2632.
20. N. Rahman, T. Kawai, G. Matsuba, K. Nishida, T. Kanaya, H. Watanabe, H. Okamoto, M. Kato, A. Usuki, M. Matsuda, K. Nakajima, N. Honma, *Macromolecules*, **2009**, 42, 4739.
21. S. Kang, S.L. Hsu, H.D. Stidham, B.P. Smith, A. Leugers, X. Yang, *Macromolecules*, **2001**, 34, 4542.
22. K. Aou, S.L. Hsu, *Macromolecules*, **2006**, 39, 3337.
23. J. Blomqvist, L.O. Pietila, B. Mannfors, *Polymer,* **2001**, 42, 109.
24. J. Blomqvist, *Polymer*, **2001**, 42, 3515.
25. T.T. Lin, X.Y. Liu, C. He, *J. Phys. Chem. B*, **2010**, 114, 3133.
26. X. Yang, S. Kang, Y. Yang, K. Aou, S.L. Hsu, *Polymer*, **2004**, 45, 4241.
27. J.L. Espartero, I. Rashkov, S.M. Li, N. Manolova, M. Vert, *Macromolecules*, **1996**, 29, 3535.

28. Hyperchem. HyperChem(TM) Molecular Modelling System, Release 4.5 SGI, Hypercube; Hyperchem(TM) Molecular Modelling System, Release 5.01 for Windows, Hypercube, Inc. (1998)
29. M.J Frisch, G.W. Trucks, H.B. Schlegel, G.E. Scuseria, M.A. Robb, J.R. Cheeseman, J. Montgomery, A.T. Vreven, K.N. Kudin, J.C. Burant, J.M. Millam, S.S. Iyengar, J. Tomasi, V. Barone, B. Mennucci, M. Cossi, G. Scalmani, N. Rega, G.A, Petersson, H. Nakatsuji, M. Hada, M. Ehara, K. Toyota, R. Fukuda, J. Hasegawa, M. Ishida, T. Nakajima, Y. Honda, O. Kitao, H. Nakai, M. Klene, X. Li, J.E. Knox, H.P. Hratchian, J.B. Cross, V. Bakken, C. Adamo, J. Jaramillo, R. Gomperts, R.E. Stratmann, O. Yazyev, A.J. Austin, R. Cammi, C. Pomelli, J.W. Ochterski, P.Y. Ayala, K. Morokuma, G.A. Voth, P. Salvador, J.J. Dannenberg, V.G. Zakrzewski, S. Dapprich, A.D. Daniels, M.C. Strain, O. Farkas, D.K. Malick, A.D. Rabuck, K. Raghavachari, J.B. Foresman, J.V. Ortiz, Q. Cui, A.G. Baboul, S. Clifford, J. Cioslowski, B.B. Stefanov, G. Liu, A. Liashenko, P. Piskorz, I. Komaromi, R.L. Martin, D.J. Fox, T. Keith, M.A. Al-Laham, C.Y. Peng, A. Nanayakkara, M. Challacombe, P.M.W. Gill, B. Johnson, W. Chen, M.W. Wong, C. Gonzalez, J.A. Pople, Gaussian 09, Gaussian, Inc., Wallingford CT, 2004. (**2009**)
30. I. Irsai, C. Majdik, A. Lupan, R. Silaghi-Dumitrescu. *Journal of Mathematical Chem*istry, **2011**, *50(4),* 703.